

332

# TRANSITIONING OF POWER FLOW IN BEAM MODELS WITH BENDS

11/10/81  
225-222

N90-24648

by

Stephen A. Hambric  
Applied Mathematics Division (184)  
David Taylor Research Center  
Bethesda, MD 20084-5000

## ABSTRACT

*The propagation of power flow through a dynamically loaded beam model with 90 degree bends is investigated using NASTRAN and McPOW. The transitioning of power flow types (axial, torsional, and flexural) is observed throughout the structure. To get accurate calculations of the torsional response of beams using NASTRAN, torsional inertia effects had to be added to the mass matrix calculation section of the program. Also, mass effects were included in the calculation of BAR forces to improve the continuity of power flow between elements. The importance of including all types of power flow in an analysis, rather than only flexural power, is indicated by the example. Trying to interpret power flow results that only consider flexural components in even a moderately complex problem will result in incorrect conclusions concerning the total power flow field.*

## INTRODUCTION

Methods for calculating power flows in dynamically loaded finite element models using NASTRAN (Rigid Format 8 - Direct Frequency Response) and McPOW (Mechanical POWER) were developed previously.<sup>1</sup> The power flow equations for beam elements derived in that paper included all forms of dynamic energy propagation: flexural, longitudinal (or axial), and torsional. The flexural waves were split into shear and moment components.

The majority of procedures employed in other studies (see the list of references in Hambric<sup>1</sup>) only consider flexural vibration in their calculations of power flow. This can be dangerous if an analyst is investigating the energy propagation characteristics of a complex structure. Though flexural vibration is in most cases the dominant response in a dynamically excited beam, different kinds of propagation will occur in structures with even a small degree of complexity, such as a simple beam model with 90-degree bends.

Such a model is tested here using a frequency range spanning several resonances and types of motion. Plots showing the contributions of the different forms of power flow to the total power travelling through the system are shown, and illustrate the importance of all types of energy propagation to the power flow method.

To improve the accuracy of both the finite element solution and the power flow solution of the problem, a few modifications were made to NASTRAN and McPOW. First, to show the importance of torsional power flow, a capability to calculate dynamic torsional forces and corresponding angular velocities is required. Therefore, torsional inertias were added to the coupled mass matrix formulation of the BAR element. Also, since the beam element force calculation algorithm in NASTRAN considers only stiffness effects, mass and damping effects had to be added to McPOW to modify the element forces.

## METHODOLOGY

The procedure for solving for the power flow field in a finite element model using NASTRAN and McPOW is:

1. Run Rigid Format 8 (Direct Frequency Response) on a NASTRAN data deck (using the ALTER statements shown in Ref. 1 to output force and velocity data blocks to the OUTPUT2 file). Coupled mass formulations should always be used.
2. Run McPOW using the binary data in the OUTPUT2 file as input.

### General Methods

A typical power flow cycle is shown in Fig. 1. The figure shows an arbitrary structure mounted to a connecting structure by a spring and damper coupling. A dynamic load is applied, and energy flows into the structure at the load point. The input power then flows through the structure along multiple flow paths denoted by arrows whose lengths represent power flow magnitudes. As the energy flows toward the mounting, it is dissipated by material damping and sound radiation into a surrounding medium, and the flow arrows shorten. The flow and dissipation processes continue until the remaining energy exits the structure through the mounting and flows into the connecting structure. Though only one power entry point and one exit point are shown in this drawing, multiple loads and mountings may exist. A classic text which describes the flow of structure-borne sound is the book by Cremer, Heckl, and Ungar.<sup>2</sup>

The structural dynamics problem may be solved using NASTRAN. The structure may be modeled with various element types; mountings are modeled with scalar spring, damping, and mass elements. Constraints and loads are directly applied. The steady-state response for the model is solved for a given excitation frequency, and the power flow variables are calculated.

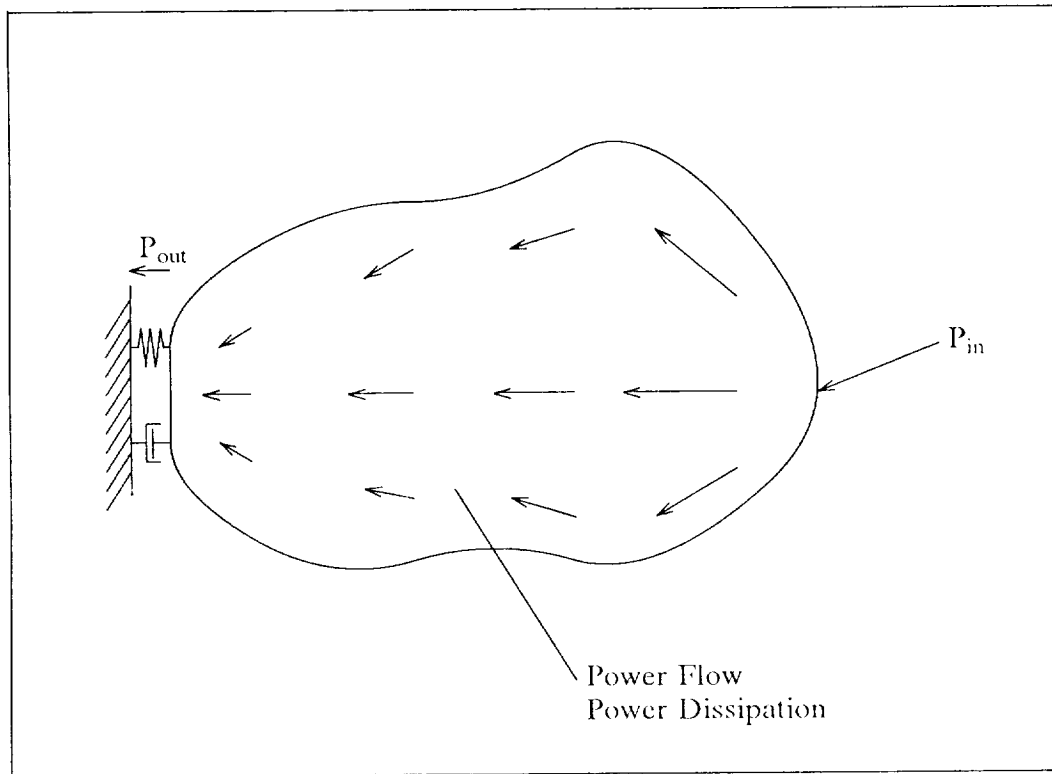


Fig. 1. Sample Power Flow Diagram.

Power is defined as the time-averaged product of a force with the in-phase component of velocity in the direction of the force. For time-harmonic analysis, where complex numbers are used, this calculation may be visualized as taking the dot product of the force and velocity phasors. (There is no factor 1/2 in the following power equations if the assumption that forces and velocities are "effective" values rather than amplitudes is made. With this assumption, consistency is maintained, and there is no mixing of effective and peak quantities in this formulation.)

Multiplying one complex number by the in-phase part of another complex number is the same operation as multiplying the first number by the complex conjugate of the other number and taking the real part of the result. Therefore a general formula for power flow in a structure is

$$\text{Power} = \text{Real} [F \cdot v^*], \quad (1)$$

where

$F$  = force, and  
 $v^*$  = complex conjugate of velocity.

### Power Flow Equations

The equations for power flows in BAR elements are repeated here. A diagram of the BAR element and its NASTRAN force output conventions is shown in Fig. 2, where Plane 1 is vertical and Plane 2 is horizontal.

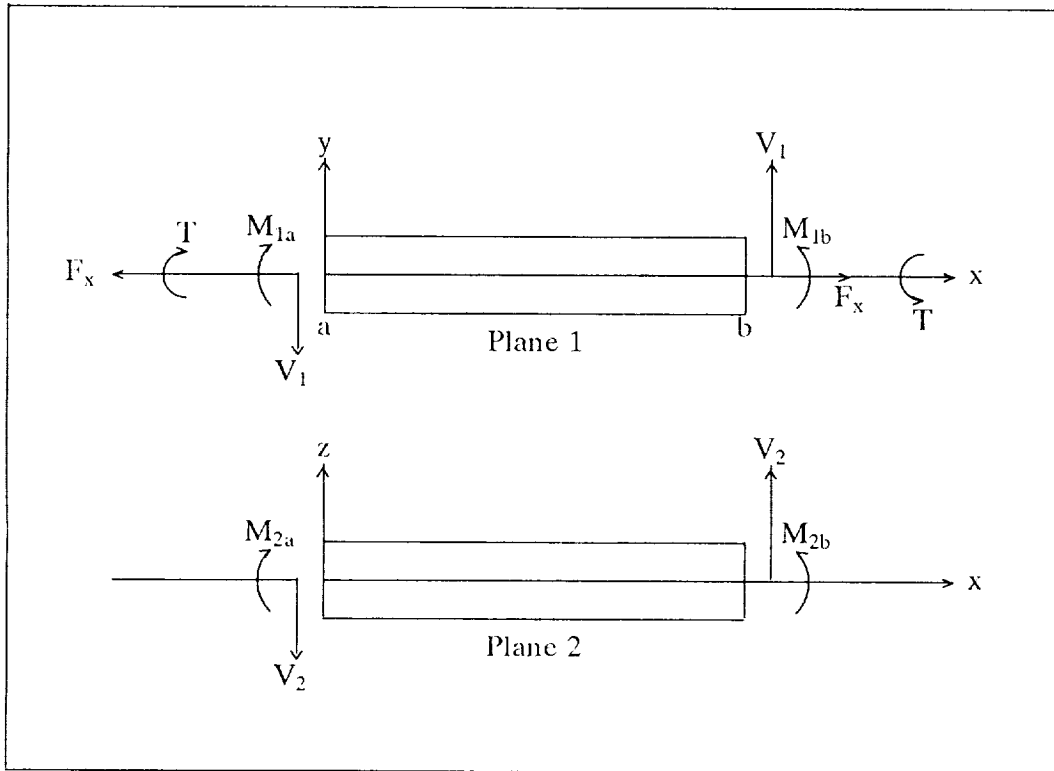


Fig. 2. The BAR Element

Since a beam is a one-dimensional element, energy flows in only one direction: in the local \$x\$ direction, or along the length of the beam. The total power flow for a beam element is

$$P_x = \text{Real} [ - (F_x v_x^* + V_1 v_y^* + V_2 v_z^* + T \dot{\theta}_x^* - M_2 \dot{\theta}_y^* + M_1 \dot{\theta}_z^*) ], \quad (2)$$

where

- $F_x$  = axial force,
- $V_1$  = shear force in \$y\$ direction,
- $V_2$  = shear force in \$z\$ direction,
- $T$  = torsion about \$x\$,
- $M_2$  = bending moment about \$y\$,
- $M_1$  = bending moment about \$z\$,
- $v_i$  = translational velocities in direction \$i\$, and

$\dot{\theta}_i$  = rotational velocities about axis i.

The negative sign on the result comes from force and displacement direction conventions for the element. The negative sign on the  $M_2$  term reflects the NASTRAN force output convention. In Fig. 2,  $M_2$  is shown as positive in the opposite sense to  $\dot{\theta}_y$ . Therefore,  $M_2\dot{\theta}_y^*$  is opposite in sign to the other power flow components.

### **NASTRAN Modifications**

#### *Torsional Inertias*

NASTRAN currently does not consider torsional inertias in its beam element formulation. Therefore, all torsional results (angular displacements and torques) are based on stiffness only, and are essentially those of a static problem solution. To remedy this, torsional inertias were added to the coupled mass formulation. At the point in NASTRAN where the basic element mass matrix is formed, no consideration is given to beam offsets or beam orientation; all mass coefficients (as well as stiffness) are calculated in the local beam coordinate system.

The torsional mass moment of inertia of a beam is  $\rho L J_x/2$ , where  $\rho$  is the mass density,  $L$  is the beam length, and  $J_x$  is the polar area moment of inertia. In the standard consistent mass matrix for a beam,<sup>3</sup> this value is broken up into 2/3 and 1/3 components; 2/3 of the value is placed at the diagonal, and 1/3 is placed at the coupled degree of freedom (the node on the other end of the beam). The same fractions are used for the translational, or axial masses. In NASTRAN, however, the coupled mass formulation uses an average of lumped and consistent formulations to reduce error. This average changes the components to 5/6 and 1/6 of the total value. Since these values are currently used for the axial masses in NASTRAN, they were also used for the torsional inertias.

#### *Element Force Calculations*

NASTRAN element forces are currently calculated by multiplying element stiffness matrices by element displacement vectors. Both damping and mass effects are ignored. The damping in a stiffness element is actually in the form of a loss factor, which generates a complex stiffness matrix. All stiffness terms are multiplied by  $1.0 + i\eta$ . For most dynamic analyses, neglecting the  $i\eta$  term is acceptable since it is generally small. For a power flow analysis of a highly reverberant structure, however, ignoring the loss factor is disastrous. In a highly reverberant structure, the force and velocity at a given point are close to 90 degrees out of phase. Since power flow is defined as the dot product of these two components, a small change in the phase of the force has large effects on the calculated element powers.

Neglecting the element mass matrices, whose components are several orders of magnitude less than those of the stiffness matrices, has less drastic

effects on the power flow solution, since at low frequencies the masses will have little effect on the force calculations (the element mass matrix is multiplied by  $-\omega^2$  to take the second time derivative of the corresponding displacements). However, when high frequency analyses are performed on a model, the  $-\omega^2$  multiplying factor becomes more significant, and neglecting the mass contributions will cause some error in the force calculations. Errors in element forces cause errors in element power flows.

Including these missing effects in NASTRAN is complicated by the fact that the element force calculation algorithm splits the problem into real and imaginary parts. The element stiffness matrices are multiplied by the real parts of the displacement vectors to calculate real force components, and the process is repeated for the imaginary components. Adding an imaginary term to the stiffness matrices causes new terms to be generated in the multiplication (imaginary stiffness x imaginary displacement and imaginary stiffness x real displacement). There is also no frequency dependence in the current algorithm, since stiffness are frequency independent. Mass matrices, however, must be multiplied by the  $-\omega^2$  term mentioned above, so they must be recalculated for every frequency.

To avoid these complications, the element force calculations were temporarily moved to McPOW. The element mass and complex stiffness matrices are recalculated on a local element level, and combined with local element displacements to solve for element forces. A force vector with 12 entries is the result; shears in the local y and z directions, moments about the local y and z directions, axial forces, and torques are solved for at each grid point. In NASTRAN only eight forces are calculated, because only moments are calculated at both ends of a beam element. Beam power flows are therefore calculated at each end of the element using only the forces at that end and the corresponding grid velocities. The average of the powers at the ends is taken to find an element power flow.

## TEST PROBLEM

### Problem Statement

The beam model that was analyzed is shown in Fig. 3. All three sections have the same cross section and material properties. Dashpots (DAMP2 elements) of value  $10^6$  were applied at the model's end in all six degrees of freedom. A unit load was applied at the top end of the model in the longitudinal direction (along the - z axis) over a frequency range of 1 to 250 Hz swept in 1 Hz increments. The finite element model consists of 152 elements and 153 grid points. Grid and element numbering starts at the left end of Link 1 and proceeds up to the end of Link 3.

Using the local beam element coordinate systems shown in Fig. 3, the following table of force balances at the corners (Link 3 to Link 2, Link 2 to Link 1) was generated.

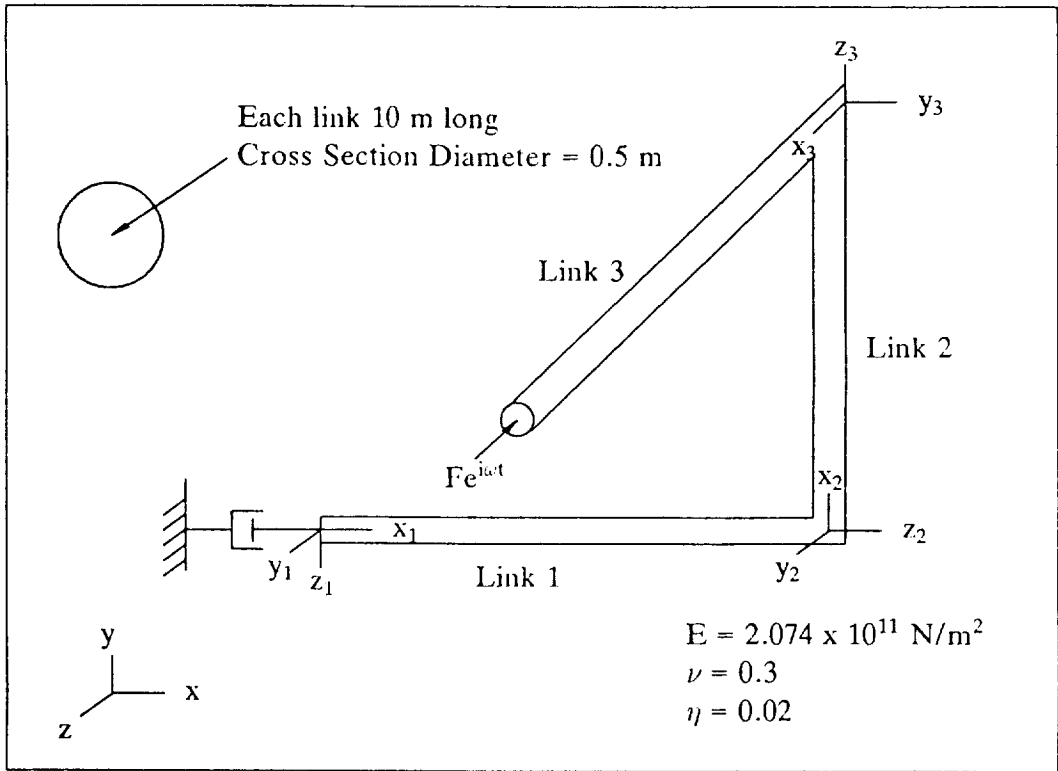


Fig. 3. Test Problem Geometry

Link 3	Link 2	Link 1
$F_x$	$V_1$	$V_1$
$T$	$M_2$	$M_2$
$V_1$	$V_2$	$F_x$
$V_2$	$F_x$	$V_2$
$M_1$	$T$	$M_1$
$M_2$	$M_1$	$T$

The subscripts on the shears and moments refer to the plane in which the forces occur (see Fig. 2). This table can be used to track the propagation of power flow through the structure. For example, the longitudinal power input to Link 3 will travel down the beam in axial waves to the first bend and become shear power flow in the z direction in Link 2. This shear power will interchange with moment power along the beam (the sum of the shear and moment components is the total flexural power flow in the beam). Any shear power that exists at the lower end of Link 2 will transition to more shear power in Link 1.

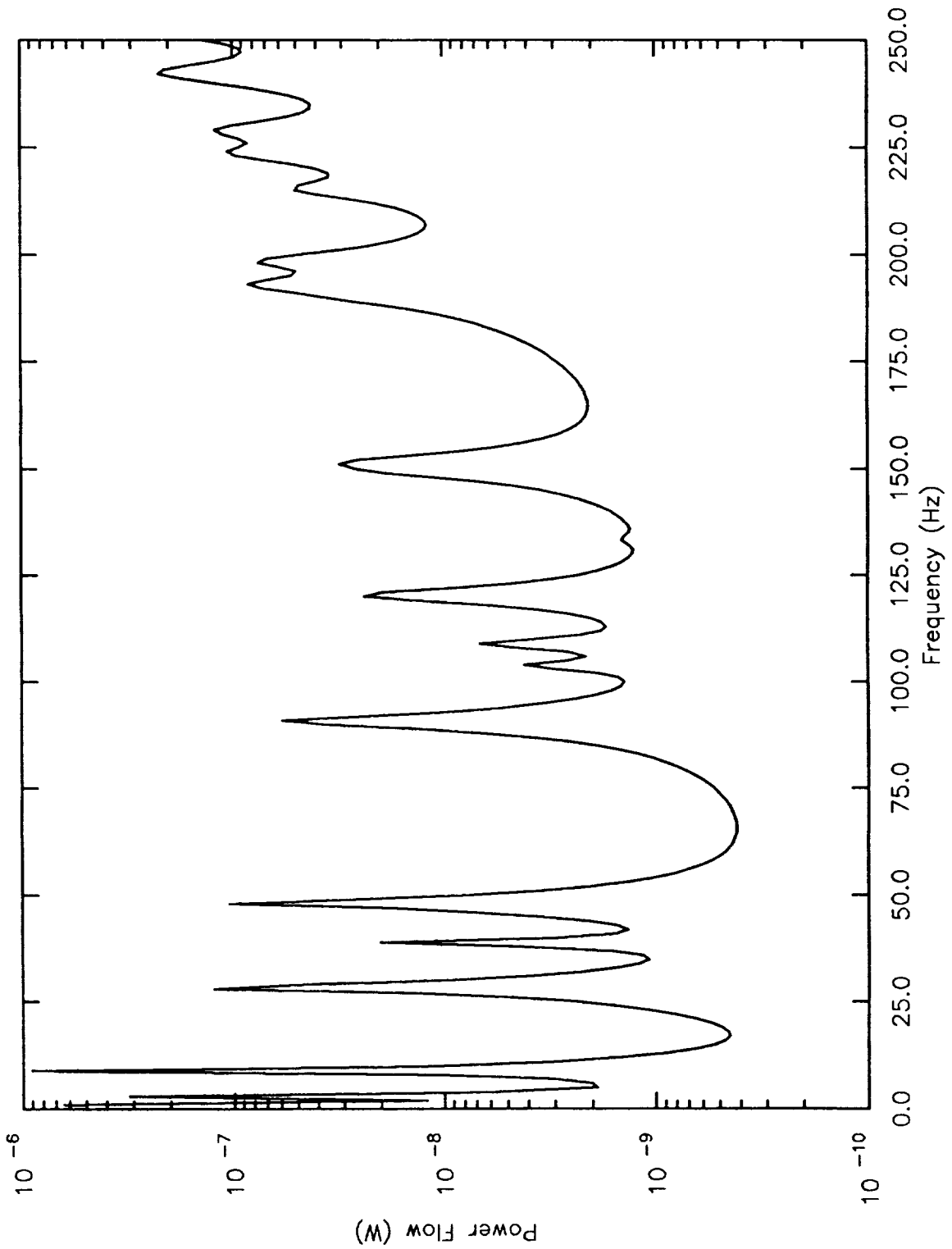


Fig. 4. Power inputs for test problem.

## Results and Discussion

The computed power input curve over the excitation frequency range is shown in Fig. 4. The power input peaks correspond to various resonances in the structure. Most are flexural, but some axial and torsional modes influence the power input curve. The longitudinal modes of Link 3 cause power input peaks (at 190 Hz and above), as well as the torsional modes of Link 1 (at 151 Hz and above).

In this model, the power flow path is independent of frequency. The total power must always flow from the input point at the end of Link 3 to the dampers at the beginning of Link 1. This simplifies the interpretation of the results, since the directions of total power flow are established.

The types of power flow in a given link are not so well-defined. Whether the dominant path in a link is flexural, axial, or torsional, depends on the motion of the structure. Fig. 5 shows the two most common types of motion paths for this problem. The displacement field of Diagram 1 occurs most often. The axial load applied to Link 3 drives the entire structure forward and backward over a frequency cycle. The dominant power flow in Link 3 is axial; the dominant power flow in Link 2 is flexural; and torsional and flexural power flows are dominant in Link 1, since the input load applies both a torque and bending moment to the link.

In Diagram 2 of Fig. 5 a different type of motion is shown. The axial load still drives the upper half of the structure in the same direction, but the lower half moves in the opposite direction. This type of motion is not what one would expect in a static problem, but the dynamic characteristics of the structure produce this type of motion in various frequency ranges.

Due to this motion path, the axial power flow travelling down Link 3 becomes flexural, torsional, and axial in Link 2. The torsional and axial components appear because the link is twisted and stretched by the opposite directions of motion of the two ends. The torsional power in Link 2 becomes flexural power in Plane 1 in Link 1, and the axial power in Link 2 turns into flexural power in Plane 2 in Link 1. The flexural power in Link 2 becomes torsional and flexural power in Link 1 as before (Diagram 1).

Considering these modes of power transitioning, the power flow plots in Figs. 6-8 may be interpreted. Each plot shows the contributions of flexural, torsional, and axial power flow as a percentage of the total power flow in the center of each link.

Fig. 8 shows the power components in Link 3. Since the input power is in the longitudinal direction, the majority of the power in this link is axial. At certain frequencies, the percentage of axial power is greater than 100 percent. The large axial percentage arises because at certain frequencies, reflected waves carry power in the opposite direction (toward the load). Three flexural resonances in the structure cause reflected power just before 50 Hz, along with

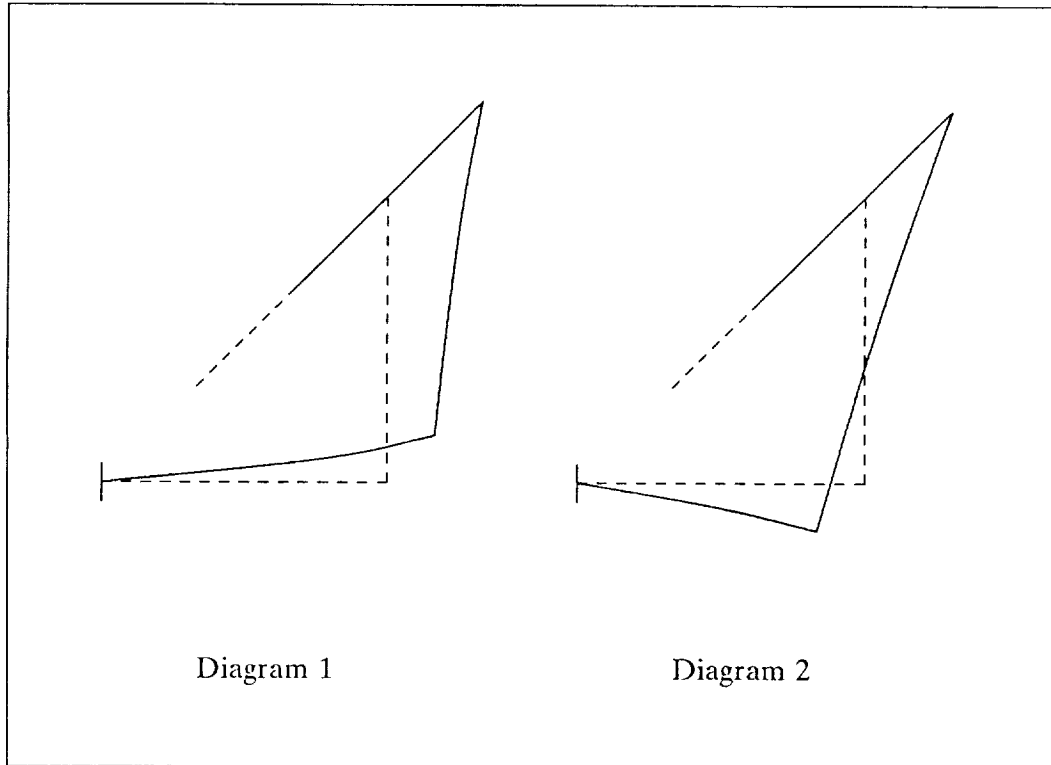


Fig. 5. Dominant motion paths for test problem

five others right after 100 Hz. Between 200 and 250 Hz, some flexural and torsional resonances cause more reflected powers.

Fig. 7 shows the power components in Link 2. The dominant type of power is the flexural component in Plane 1, and is denoted by the solid curve. This type of power field corresponds to the motion type shown in Diagram 1 in Fig. 5. However at certain frequencies, the power flow pattern of Diagram 2 becomes dominant, and axial and torsional power become important. In most cases, the axial power flows forward (away from the load point), and the torsional power is backward (reflected toward the load point). These tendencies occur at the same frequencies as the reflected power waves do in Link 3 (shown in Fig. 8). This behavior indicates that the flexural power in Plane 1 and the torsional power cause reflected flexural powers in Planes 2 and 1 respectively in Link 3.

Fig. 6 shows the power distribution in Link 1. In this case, all power components are positive, implying that the reflected power waves in Links 2 and 3 originate from the joint connecting Links 1 and 2. In Link 1, flexure in Plane 1 and torsion are the dominant components of power flow. Flexural

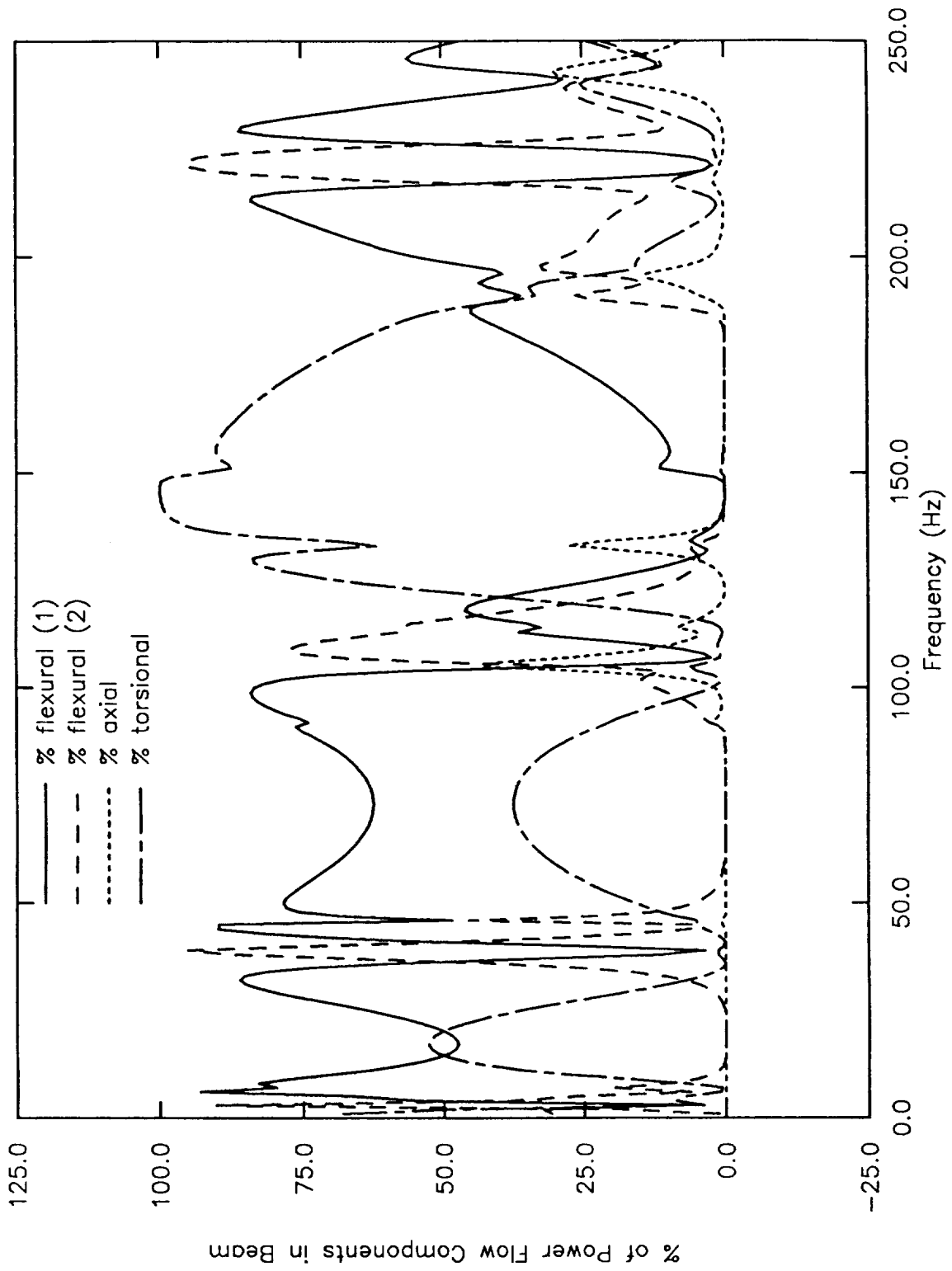


Fig. 6. Power flow types in Link 1.

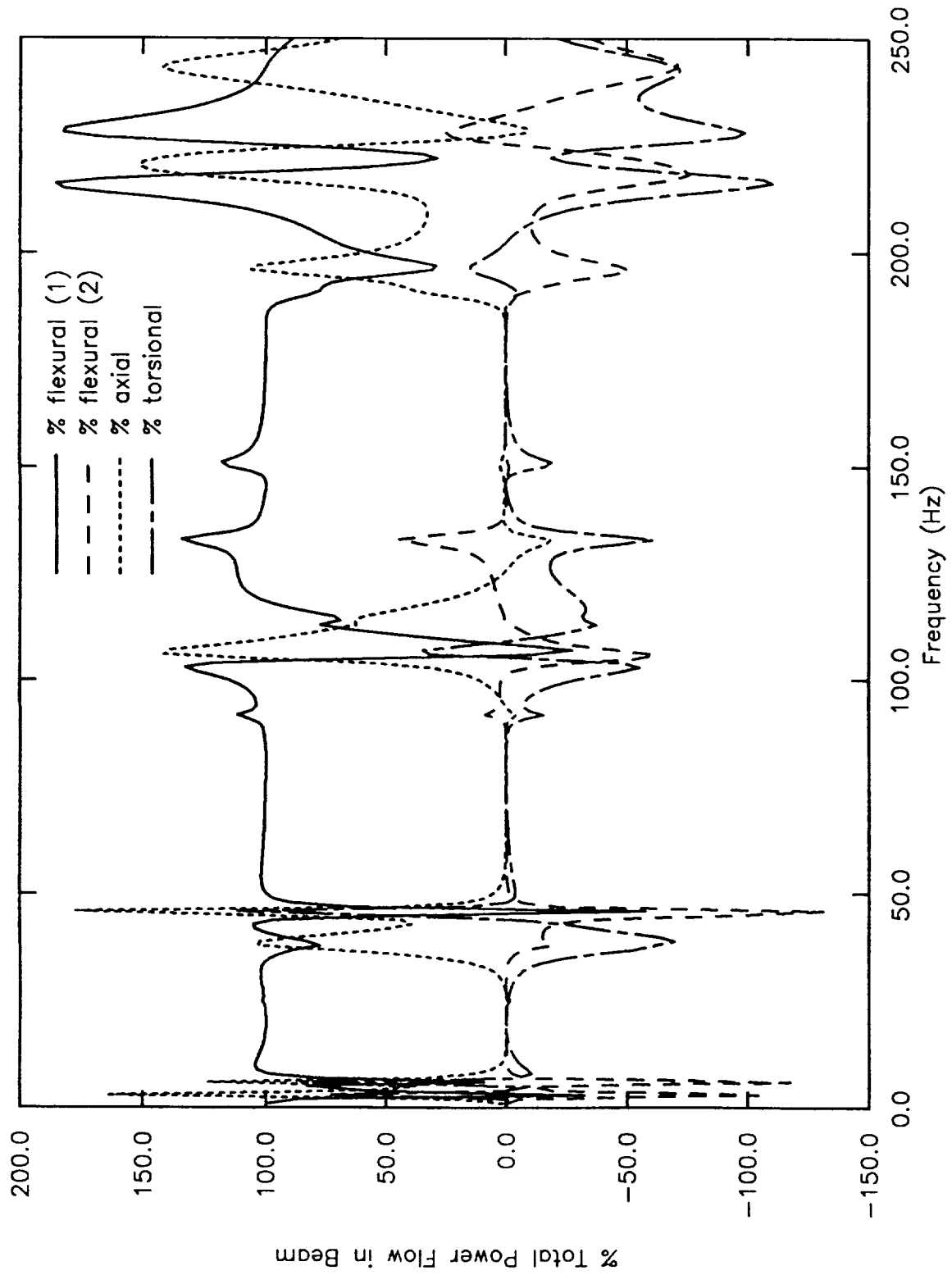


Fig. 7. Power flow types in Link 2.

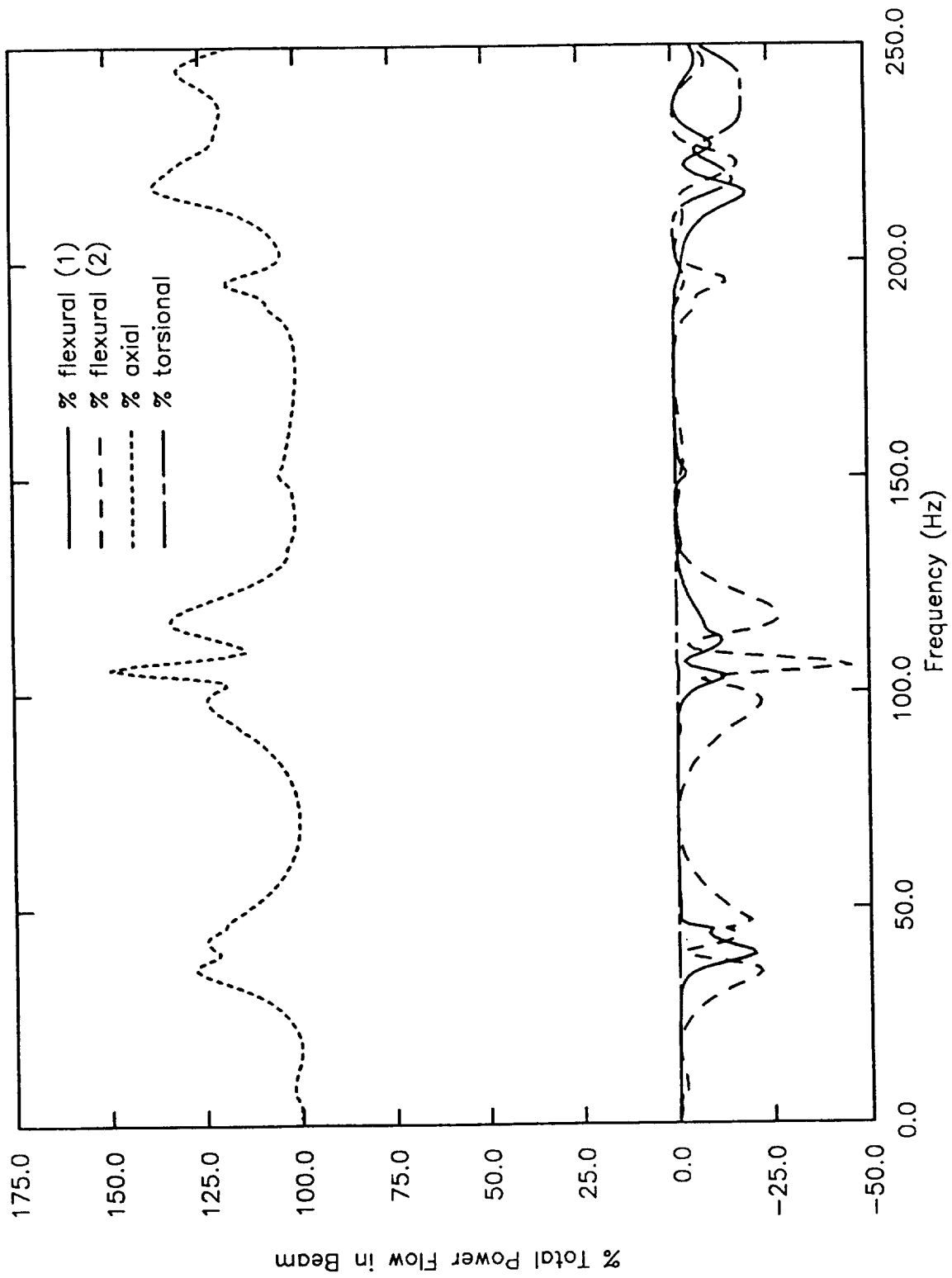


Fig. 8. Power flow types in Link 3.

motion in Plane 2 and axial motion cause power peaks at the same frequencies observed in Figs. 7 and 8, indicating the type of motion shown in Diagram 2 in Fig. 5. A torsional mode in Link 1 accounts for the peak in the torsion curve at 150 Hz, along with an input power peak at the same frequency (see Fig. 4).

In spite of the large variation in percentages of power types in the plots, all the power curves add up to 100 percent, as expected. In addition, the total power flow in the structure at all frequencies is at a maximum at the load point, and smoothly decreases to a minimum at the connection point to the dampers. The steady decrease in power is due to structural damping. The remaining power is all dissipated by the connected dampers.

This example illustrates the importance of all types of power components in a power flow analysis. Imagine trying to discern a meaningful power flow field from only flexural powers in this example. The detected powers in Link 3, which is adjacent to the input load, are all in the opposite direction, or toward the load. In Link 2, the analyst would see a sudden jump in power to values that are higher than that of the input power. Finally, in Link 1, sporadic power curves with values near the input power at frequencies below 100 Hz and values near zero after 100 Hz would be found. Confusion would surely result, with erroneous conclusions soon following. Difficulties like these would be compounded in a real application with some degree of complexity.

## CONCLUSIONS

The modifications made to NASTRAN and McPOW are critical to the power flow method. Without torsional inertias applied to the beam element mass matrices, any torsional effects in a dynamic problem are static. None of the torsional power flows present in the example problem would exist, causing incorrect total power flow fields. Adding mass and damping effects to the element force calculation algorithm is also important. In a reverberant structure where forces and velocities are nearly 90 degrees out of phase with each other, accurate calculations are necessary to guarantee good power flow results. A small change in the phase of an element force, caused by neglecting the material loss factor, could cause large errors in element power flows. Also, at higher frequencies, element mass terms can become significant and affect the element force magnitudes, and hence the element power magnitudes.

The addition of torsional inertia to the beam element mass matrix formulation was straight-forward. The addition of damping and mass effects to the element force calculation routines, however, was almost impossible. In fact, the changes had to be made to McPOW instead of NASTRAN. The implementation difficulties were due to the way NASTRAN handles complex analysis: the solutions are broken into real and imaginary parts. When the program was in its formative stages, UNIVAC computers were supported.

The UNIVAC, unfortunately, had no way of handling double precision complex arithmetic. Therefore, no complex numbers or FORTRAN complex functions are used in the element force calculation sections of the program. With this approach, a simple complex calculation like  $[-\omega^2 [M]_e + (1 + i\eta)[K]_e] \{d\}_e$  must be split up into four calculations. Also, since the calculation is frequency-dependent, the NASTRAN element force subroutines are not currently able to handle it. Since the UNIVAC has all but disappeared from the COSMIC NASTRAN computing arena and most modern computers support double precision complex arithmetic, perhaps the way NASTRAN handles complex problems should be modified.

The importance of including longitudinal and torsional components with flexural ones in a power flow analysis was shown in the example problem. Measuring flexural power alone will not give an accurate indication of the total power flow field in even a marginally complex problem. In the case of the example problem, reflected flexural waves actually indicated a reversal of power flow in the model, where the direction of flexural power was in the opposite direction of the input power. Trying to interpret power flow results that only consider flexural components will result in incorrect conclusions concerning the total power flow field.

#### REFERENCES

1. Hambric, S.A., 1988, "Power Flows and Mechanical Intensities using NASTRAN," Proceedings of the Seventeenth NASTRAN Users' Colloquium, pp. 262-289 (1989).
2. Cremer, L., Heckl, M., and Ungar, E.E., 1973, *Structure-Borne Sound*, Springer-Verlag, New York.
3. Przemieniecki, J.S., 1968, *Theory of Matrix Structural Analysis*, McGraw-Hill, New York.